Cadaver "Calamari" Amyloidogenic Fibrin Aggregates

Spike Protein Pathology from Cadavers Exposed to Bioengineered SARS-CoV-2

KEVIN W. MCCAIRN PH.D.
MAY 10, 2025

Kevin W. McCairn, Ph.D., Kevin McKernan Ph.D., Shojiro Kato M.D., Charles retired (USMC-CBRN)

Abstract

This report presents a preliminary forensic analysis of anomalous fibrin-like aggregates recovered from postmortem human cadaveric samples. Through a combination of gross morphological inspection, cryosection histology, fluoresce staining, scanning electron microscopy (SEM), elemental analysis (EDX), real-tim PCR, Raman spectroscopy, and Real-Time Quaking-Induced Conversion (RT-Qu the samples were examined for biochemical and ultrastructural features associat with amyloidogenic and protease-resistant fibrin formation. Findings suggest th clot samples exhibit hallmarks of abnormal protein aggregation consistent with pathological fibrin remodeling, including enhanced autofluorescence, beta-sheet domains, dense fibrillar ultrastructure, and spectral anomalies. PCR confirmed t human origin of the tissues, and preliminary evidence of molecular markers asso with recombinant spike protein exposure (SV40 & Ori) was observed. Limitations provenance, sample control, and chain-of-custody are acknowledged, and furthe

Introduction

Recent reports have drawn attention to the presence of large, rubbery, white fibr clots recovered from postmortem human vasculature. These structures have beer described anecdotally by embalmers and morticians and have raised questions regarding their origin, composition, and potential pathological significance. In response, this investigative effort sought to apply rigorous analytical methodolog determine whether these samples represent a known thrombotic phenotype or re novel features associated with emergent pathologies.

It is now broadly recognized that SARS-CoV-2 infection can exert systemic effec beyond its respiratory tropism, with evidence pointing to persistent coagulopath fibrin dysregulation. Of particular concern is the potential of the viral spike prot whether introduced via infection or recombinant delivery platforms such as LNP mRNA vaccines—to catalyze the formation of amyloid-like fibrin clots. Prior stu have demonstrated that spike exposure can induce fibrin(ogen) conformational changes that resist fibrinolysis and exhibit beta-sheet structures akin to amyloid fibrils.

This report investigates whether the cadaver-derived clots under study bear the morphological and biochemical hallmarks of such aberrant fibrin. Key research questions include: Are the structures of human origin? Do they exhibit features consistent with amyloidogenesis? Can they be differentiated from conventional f emboli or white clots found in known medical conditions?

Through a multidisciplinary forensic approach, this document catalogs the physi and biochemical attributes of the clot specimens, aiming to provide a transparen methodologically sound foundation for independent review. Given the limitation

the sampling context and absence of complete clinical background, the findings presented here are exploratory and intended to prompt further controlled researc

Section 1: Gross Morphology of Clot Structures Image: Slides 1–5
Initial macroscopic inspection of the cadaver-derived clot specimens revealed strikingly anomalous morphology. The samples appear rubbery, fibrous, and frequently coiled or banded—bearing superficial resemblance to marine calamar Unlike conventional thrombi, these aggregates lack the red-brown coloration an laminar erythrocyte-rich stratification commonly observed in postmortem clots.

Images collected at 4K resolution under dissecting microscope conditions show the structures retain a solid, tensile integrity. The specimens resist tearing, do nc collapse under moderate compression, and maintain structural coherence when manipulated, suggesting a composition distinct from typical fibrin gels. Internal sections show a dense, layered architecture without clear vascular lumens, furthe differentiating them from vessel-associated thrombi.

These morphological traits suggest either advanced cross-linking within a protei matrix or a structurally aberrant form of polymerized fibrin. The preserved integ and resistance to manipulation raise the possibility of amyloidogenic remodeling hypothesis explored in the following sections through microscopic and spectrosc analysis.

Section 2: Histology and Fluorescent Imaging of Cryosections Image: Slides 6–1
Tissue samples were cryosectioned at 20 µm thickness and subjected to light and fluorescence microscopy at both 4X and 40X magnification. Hematoxylin-free im reveals a heterogeneous, fibrous internal structure with numerous cavities and la fibrillar regions.

Fluorescence analysis prior to staining revealed strong and uniform intrinsic autofluorescence. Under blue-light excitation, green emission was observed; exci

in the green channel induced red fluorescence. This broad-spectrum response is highly atypical and suggests a high degree of intrinsic molecular ordering or aro residue stacking. Such behavior is consistent with cross-linked protein networks amyloid-like interactions involving tyrosine, tryptophan, or phenylalanine residu

Thioflavin T (ThT) staining was used to assess the presence of beta-sheet rich an domains. Comparative imaging before and after ThT application revealed discre "polka-dot" fluorescent foci, as well as diffuse interspersed fluorescence. These c indicate that amyloidogenic stacking is localized but not homogeneous, suggesti microclot heterogeneity within the sample.

Section 3: Scanning Electron Microscopy (SEM) and Elemental Composition vi EDX Image: Slides 12–17
Cryosections of 5 µm thickness were prepared for SEM. At low magnification (25 overall morphology was assessed. Higher magnifications (up to 5000X) revealed a dense reticular meshwork of fibrillar aggregates.

These fibrils display nodular topography and branching interconnections, consis with pathological protein assembly. Notably, a rotational twist and lateral aggreg features were observed, hallmarks of amyloid fibrin architecture. These ultrastru findings support the hypothesis that the observed material is not simple polymer fibrin but instead a protease-resistant, misfolded protein aggregate.

Elemental mapping via EDX revealed high abundance of carbon, nitrogen, oxyge sulfur—consistent with proteinaceous material. No significant signal was detect heavy metals (e.g., Fe, Zn, Cu), ruling out mineral-based aggregation or contamin The absence of inorganic nucleation points supports an endogenous biochemica origin.

Section 4: PCR and Raman Spectroscopy for Tissue and Molecular Signature Ir Slides 18-20

PCR using primers for the human RNAP transcript confirmed that the clot-deriv samples were of human origin. Additional assays targeting spike protein coding sequences and plasmid-related markers (SV40, Ori) revealed late-cycle amplificat consistent with trace residual presence of recombinant vaccine components. The findings are preliminary and require cautious interpretation.

Raman spectroscopy revealed a major spectral peak at ~1720 cm^{-1}, diverging from canonical amyloid beta-sheet signature near 1670 cm^{-1}. This spectral upshift may reflect altered secondary structure, ester linkage formation, or protonation of aci residues. The results point to an atypical fibril composition that may represent a polymorph or hybrid aggregate class.

Section 5: RT-QuIC Seeding Activity in Plasma Extracts

RT-QuIC analysis was used to assess seeding potential of the clot-associated mat 3D bar plot visualization of fluorescence intensity across a 96-well plate revealed elevated ThT signal in experimental wells, consistent with fibril formation, wher challenged against human plasma.

However, background signal, handling artifacts, and absence of dilution series lir interpretation. Without kinetic rate modeling and control seeding, the data rema suggestive but inconclusive for prion-like activity.

Conclusion

The clot structures described herein exhibit abnormal morphological, histologic ultrastructural, and spectroscopic features. Their dense fibrillar architecture, autofluorescence, ThT reactivity, spectral shifts, and preliminary RT-QuIC activi suggest amyloidogenic remodeling of fibrin under unknown conditions.

While the findings are not definitive, they raise substantial biosafety and pathophysiological questions that warrant immediate, controlled follow-up. The uncertain provenance and unstandardized collection methodology underscore th

need for independent replication with verified chain-of-custody.

In the current context of vaccine-induced spike protein exposure and post-infect complications, these results may point to a novel or under-recognized pathology. such, they constitute a call for interdisciplinary scientific inquiry, clinical vigilan and transparent investigation.

Slides

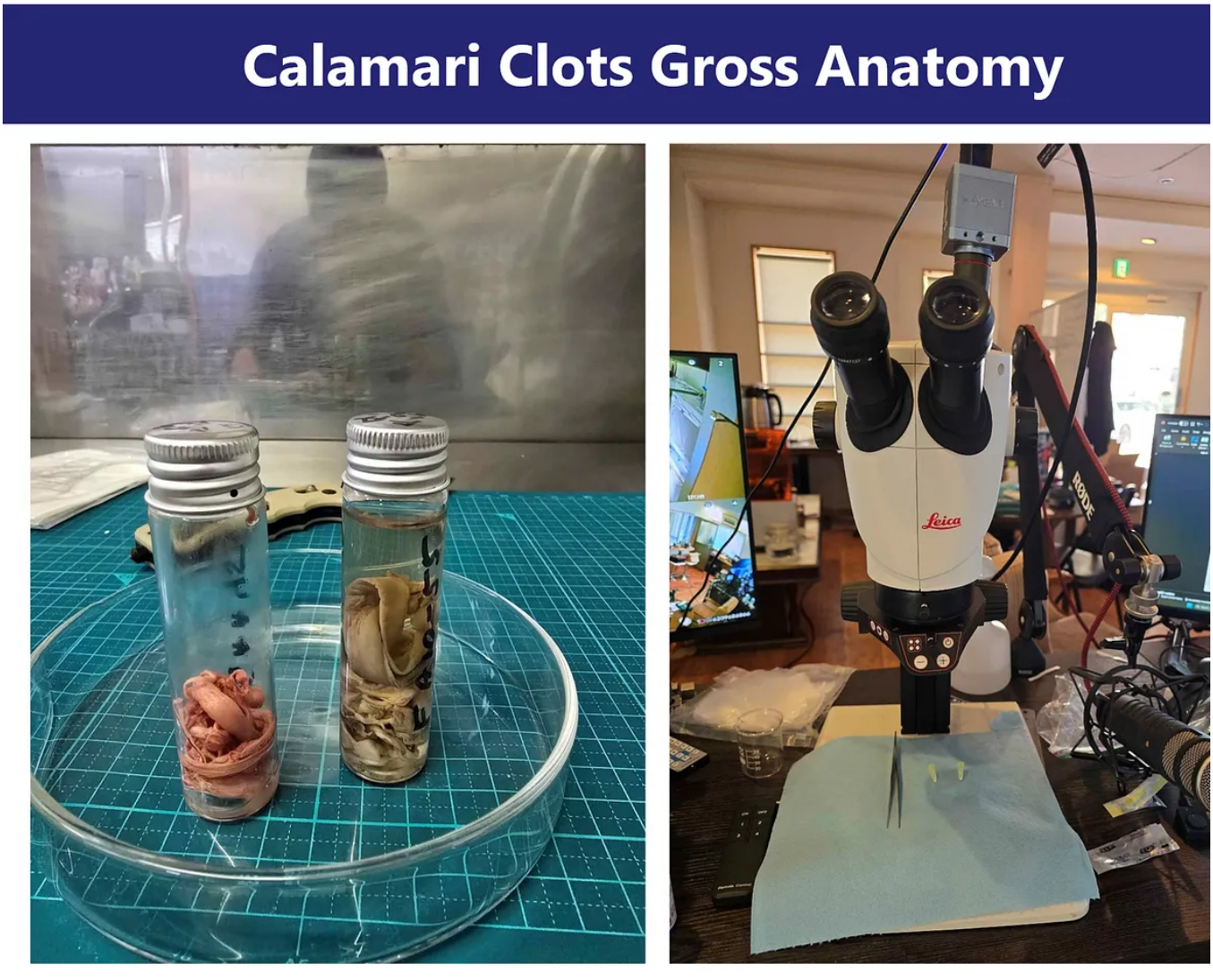

Slide1: A view of the samples as received, under argon (LHS) or formalin, the dissection of the argon stabilized clot was conducted using a laboratory grade dissecting microscope where images were collected at 4K resolution.

Slide 2 shows a sample extracted from the tube and pinned to the dissection area using two 30-gauge hypodermic needles.

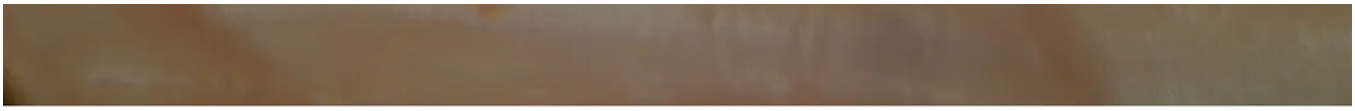

Slide 3: Shows the specimen under the dissecting microscope, there are several surface features which are present, including fissures and striations, and there appears to be a laminar type of architecture that is difficult to discern without magnification.

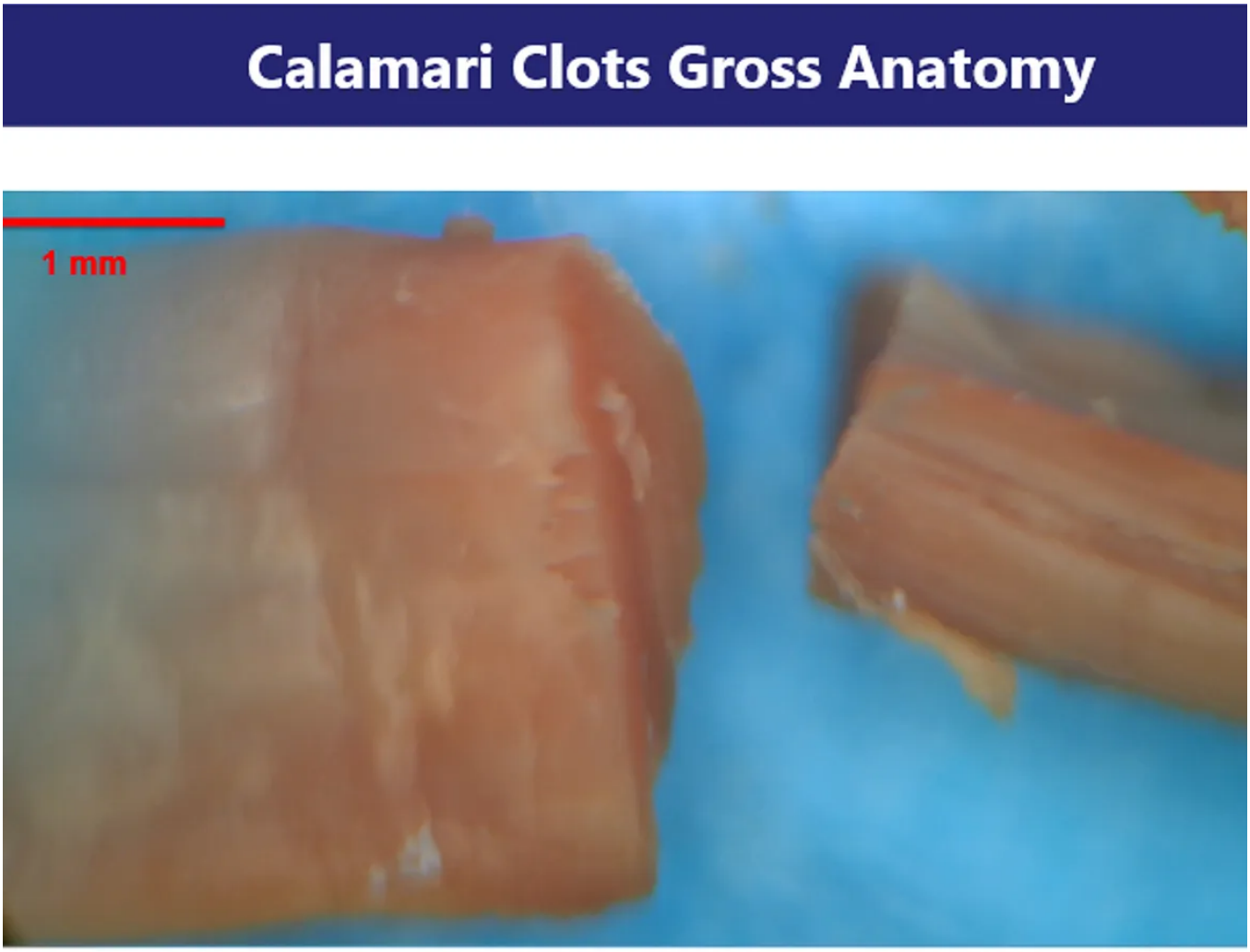

Slide 4: Shows the clot after cutting with a scalpel blade, at this scale of magnification the specimen has a solid appearance and lacks the necessary lumen were it a functional part of the vasculature.

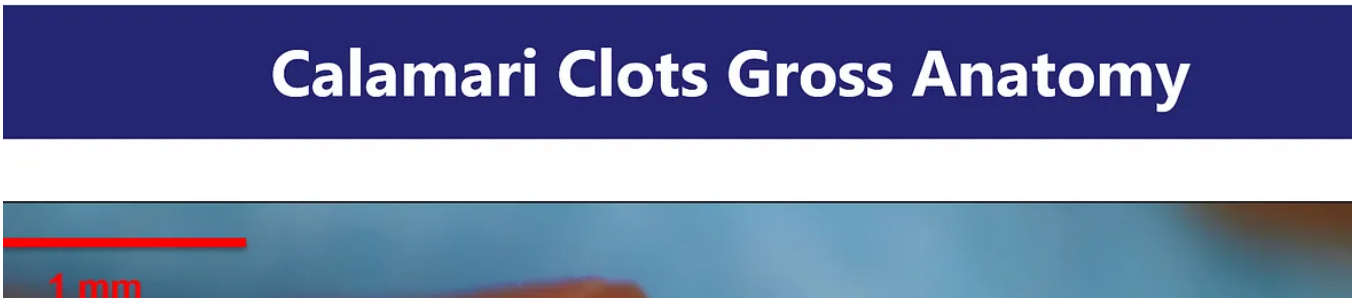

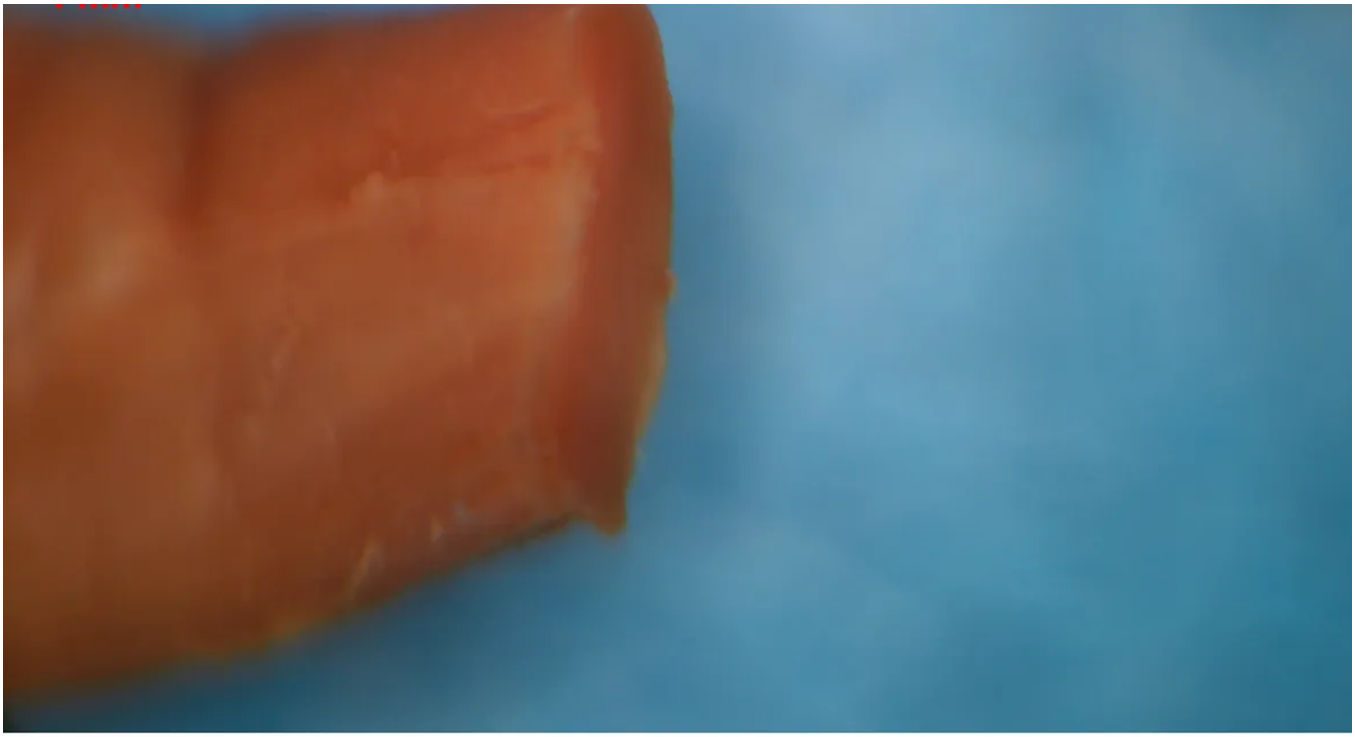

Slide 5: Shows another section of the clot after cutting with a scalpel blade, and the intensity of the lighting changed to highlight the solid appearance through the structure, and of the cut face.

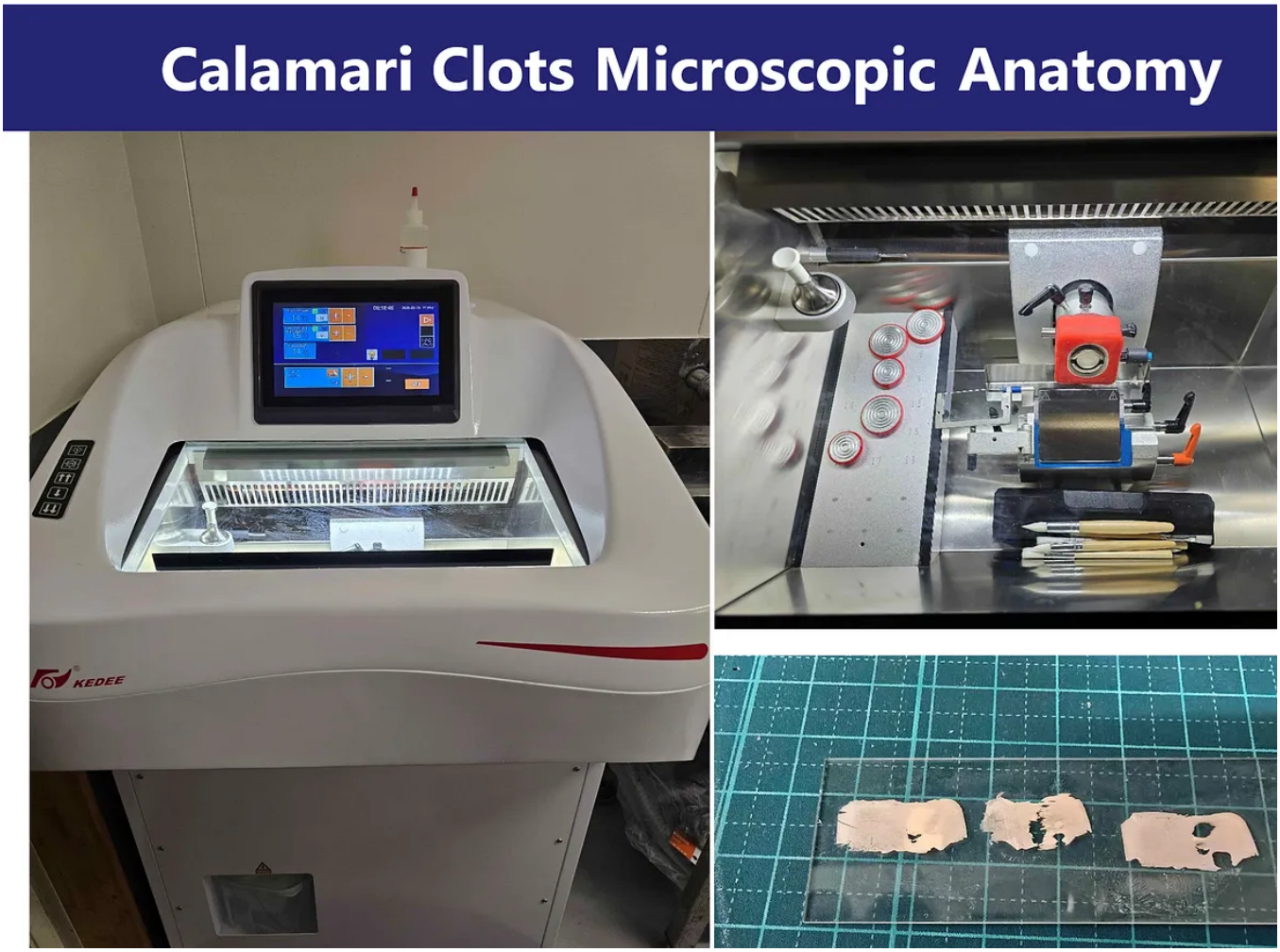

Slide 6: Showing the Cryostat used to section the tissue in question and the samples after cutting mounted to a standard glass slide.

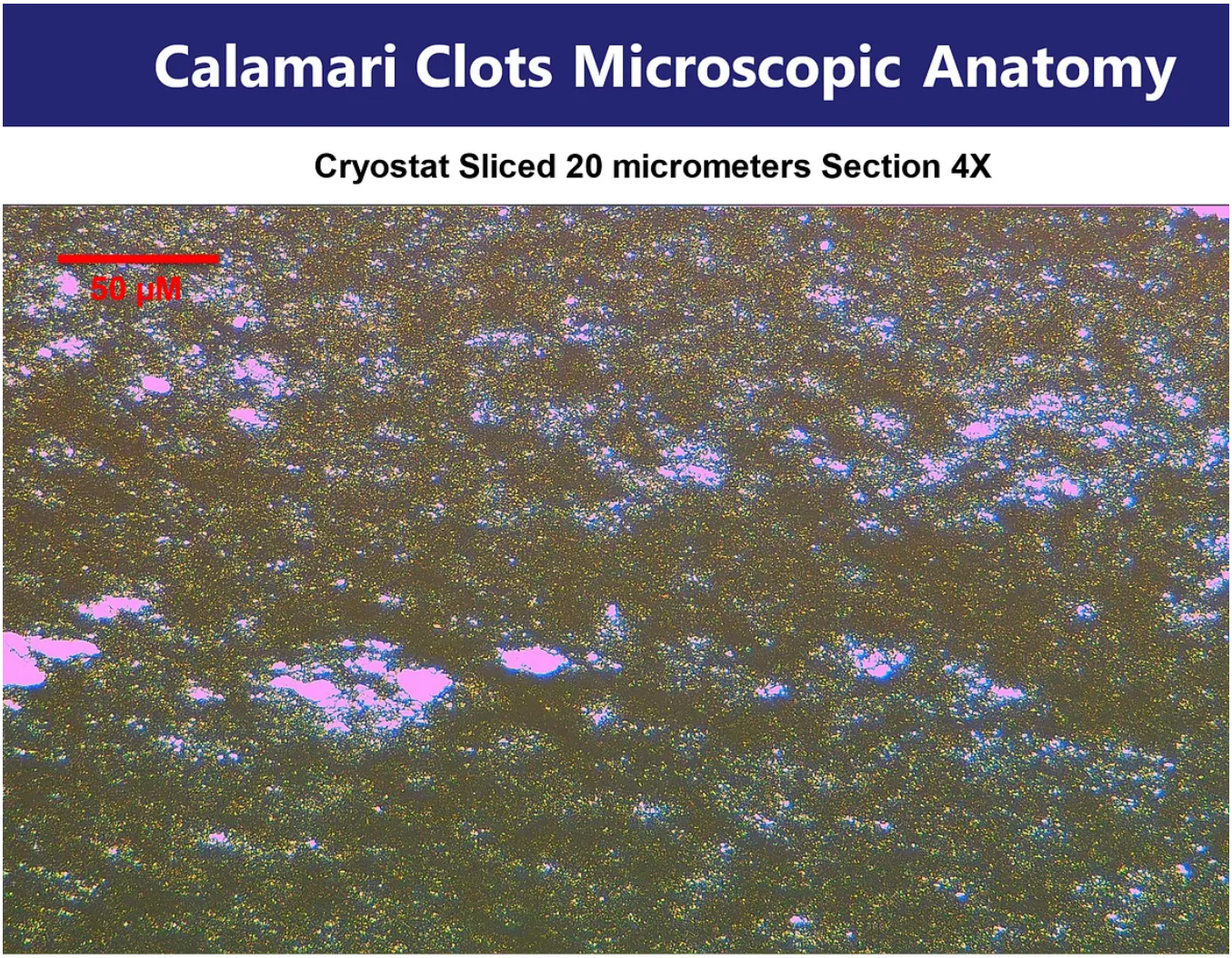

Slide 7: Low power magnification (4X) shows that the tissue is far from the solid tissue as first observed in the dissecting microscope, there are numerous cavities, and beginning of a fibrous appearance.

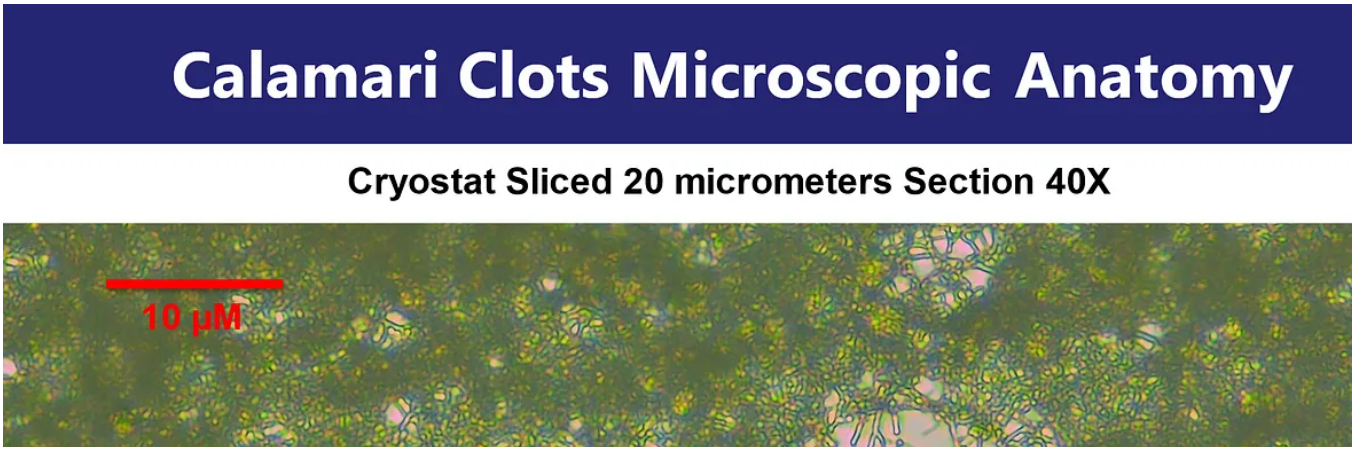

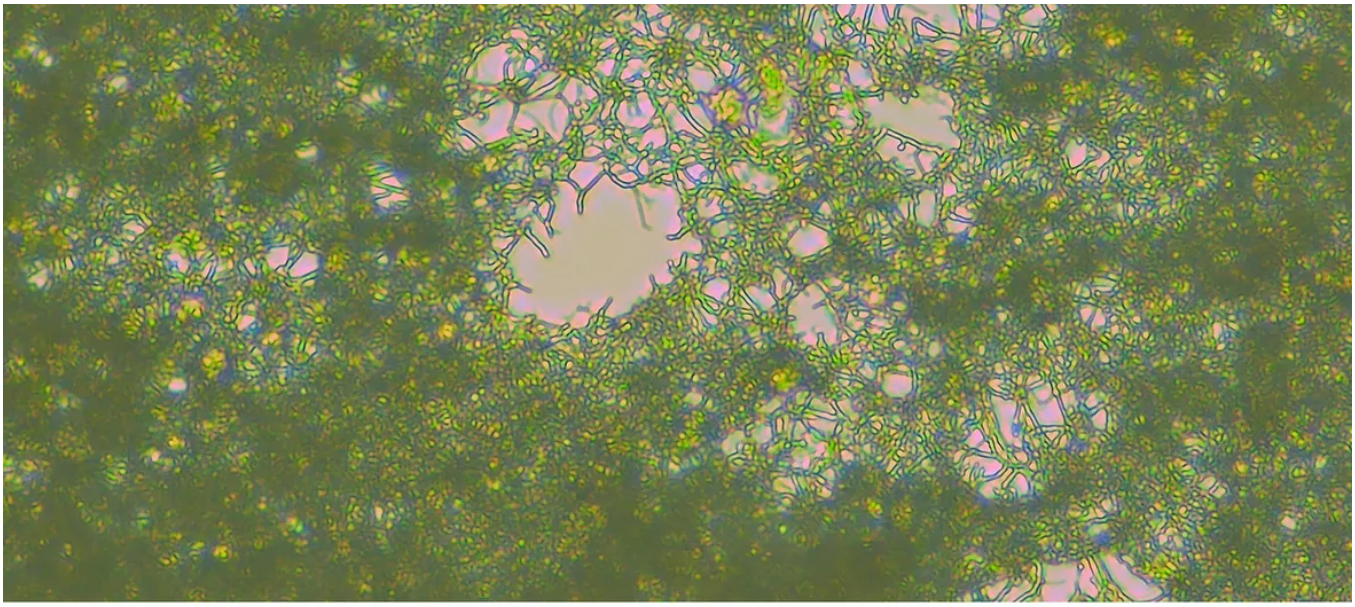

Slide 8: At higher magnification (40X) under normal light microscopy conditions a fibrous and matted appearance becomes the obvious feature.

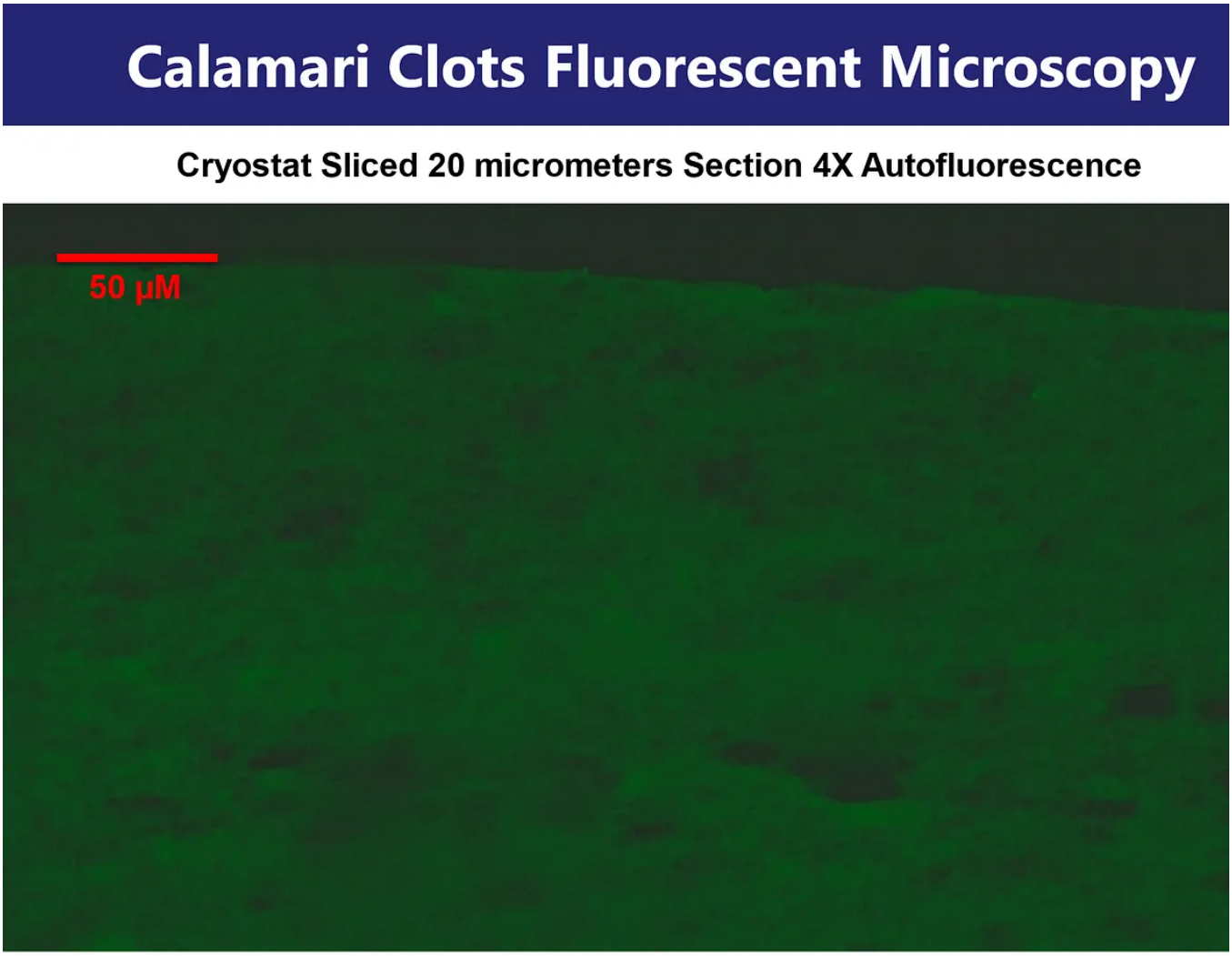

Slide 9: An example of the near uniform autofluorescence observed from the sample,

under a blue fluorescence source, which causes it to fluoresce in the green spectrum.

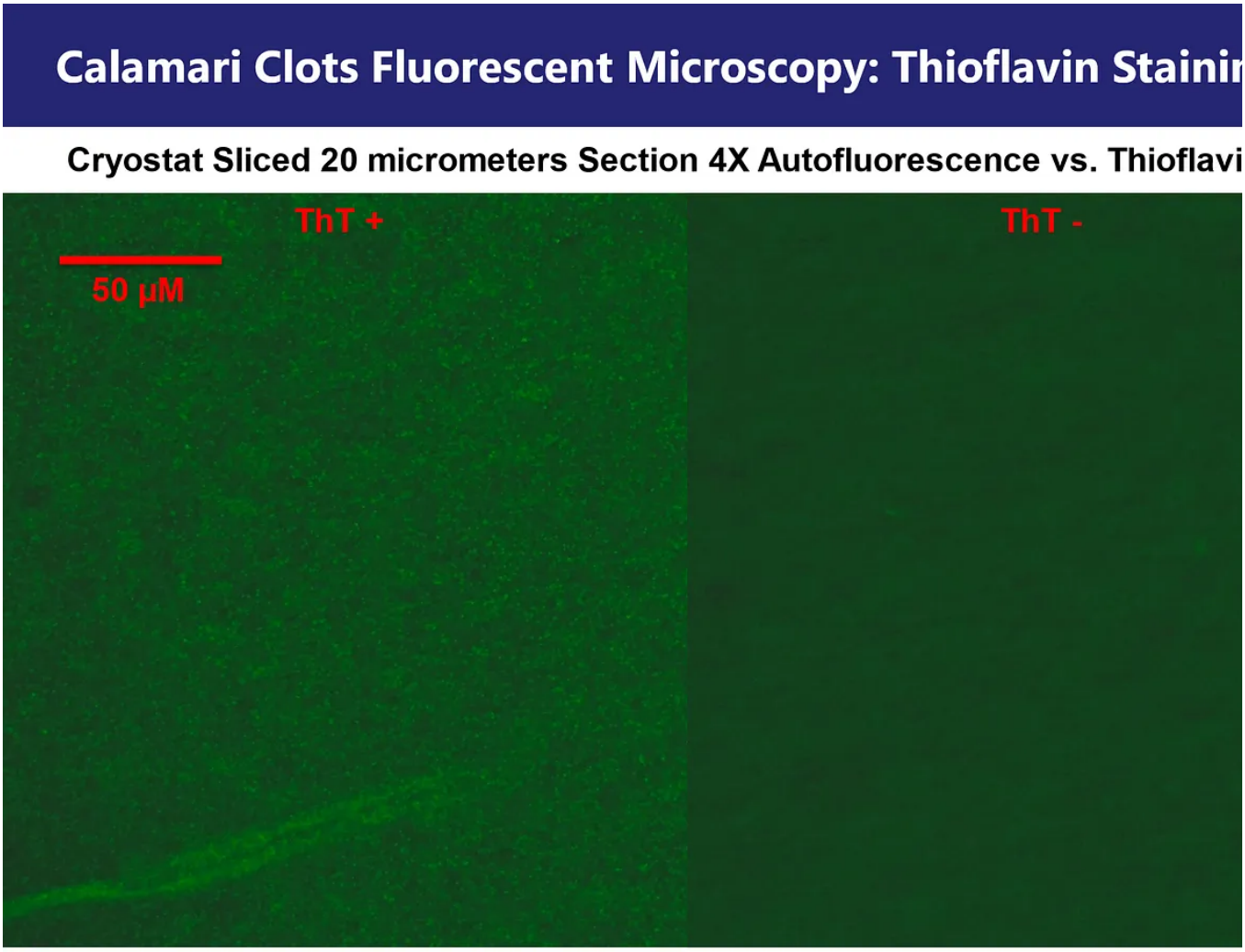

Slides 10 Show side by side comparison of the tissue in autofluorescence mode and after histological staining with ThT (left hand side), at (4X) magnification there is a distinct polka-dot appearance of areas that have taken up ThT relative to its surroundings, this would indicate that these are regions in which the amyloid stacking has occurred and are perhaps the microclots that have been reported in previous studies.

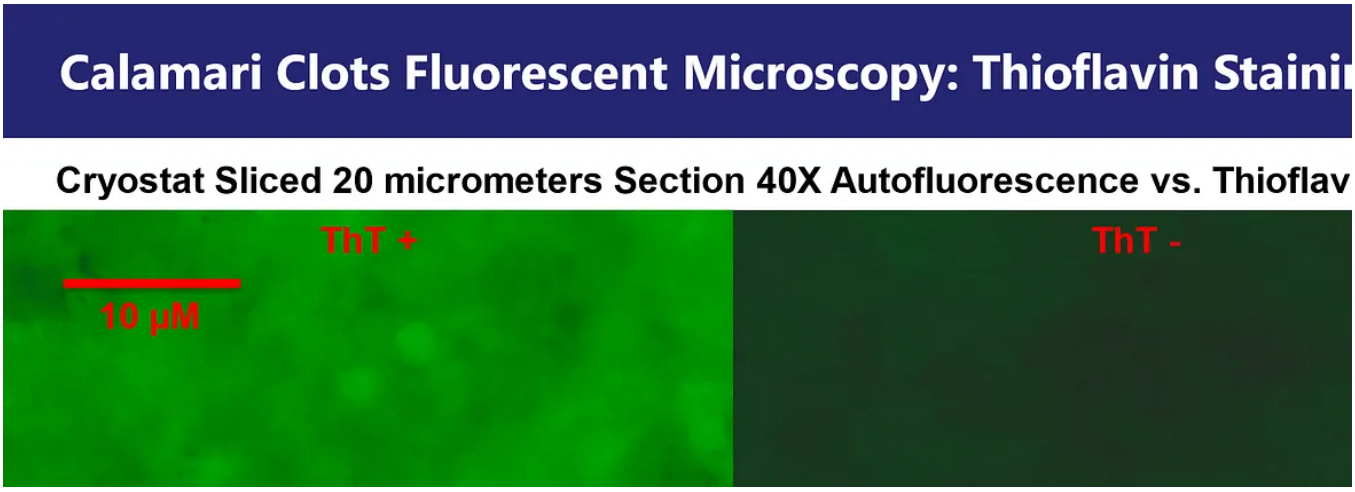

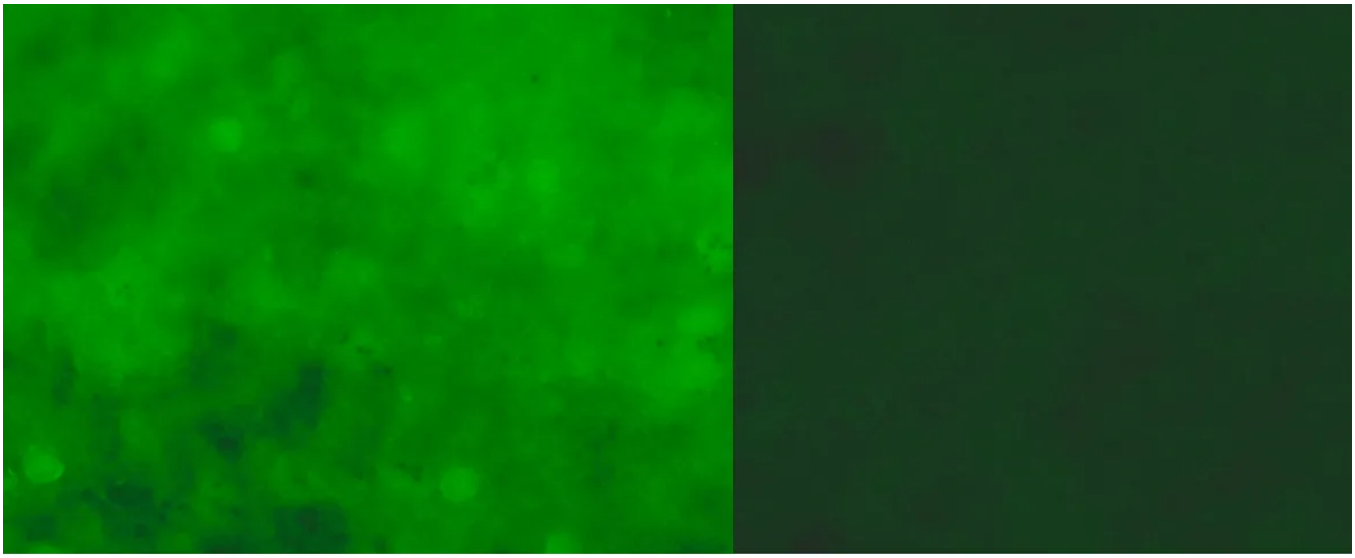

Slides 11 There is, however, a strong uptake of dye in the intervening space between areas of high concentration suggesting that these regions contain amyloidogenic material as well, this is most evident in the higher (40X) times magnification range.

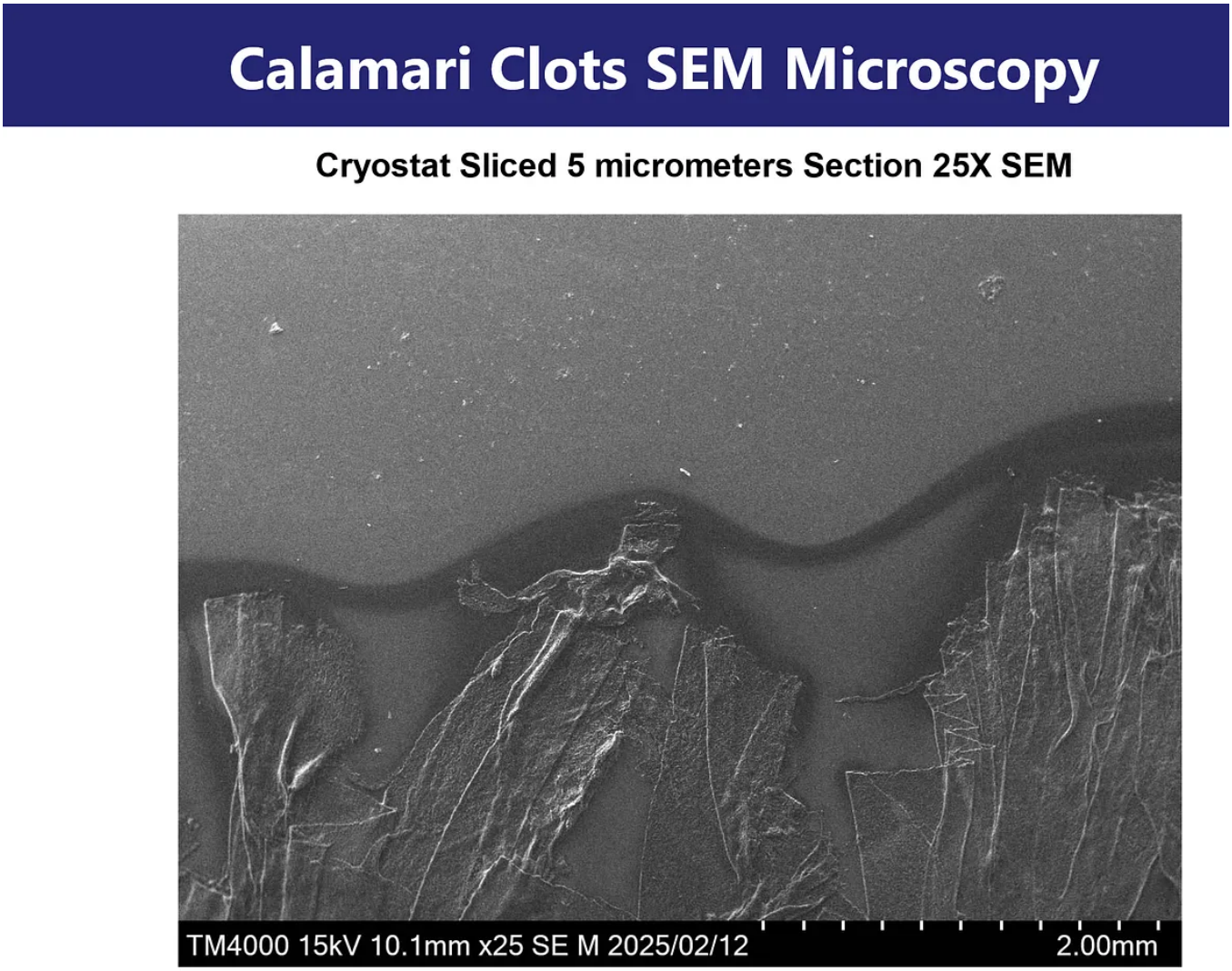

Slide 12: We now transition from using light and fluorescent microscopy to SEM,

the first image (25X) allows us to orientate ourselves to the specimen which fills the lower half of the image.

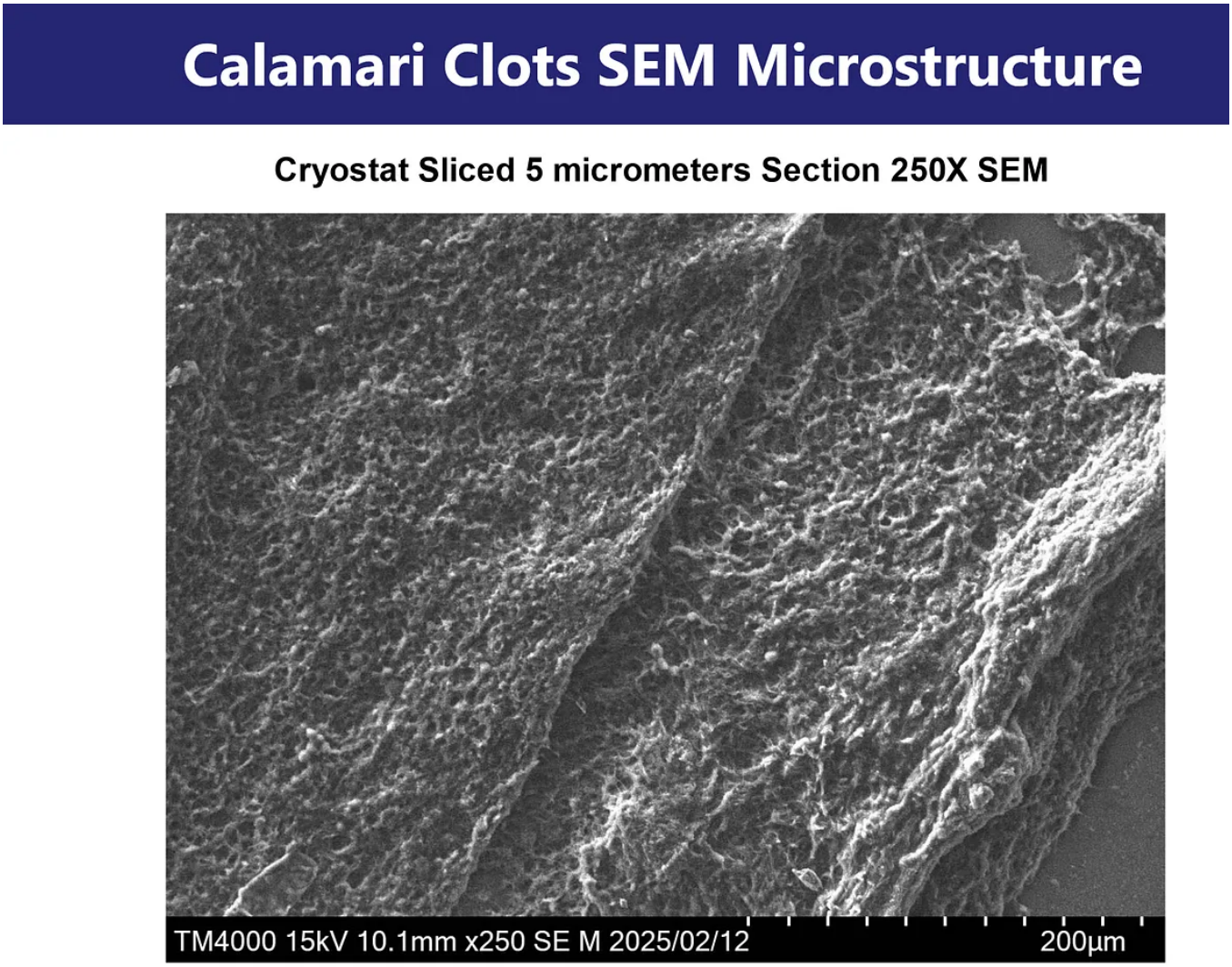

Slide 13: Transitioning to a higher magnification, we are now moving beyond the capabilities of light microscopy and one fiber of the clot forms the image in this slide. A nodular appearance, transposed onto linear topology begins to become apparent at this scale of magnification.

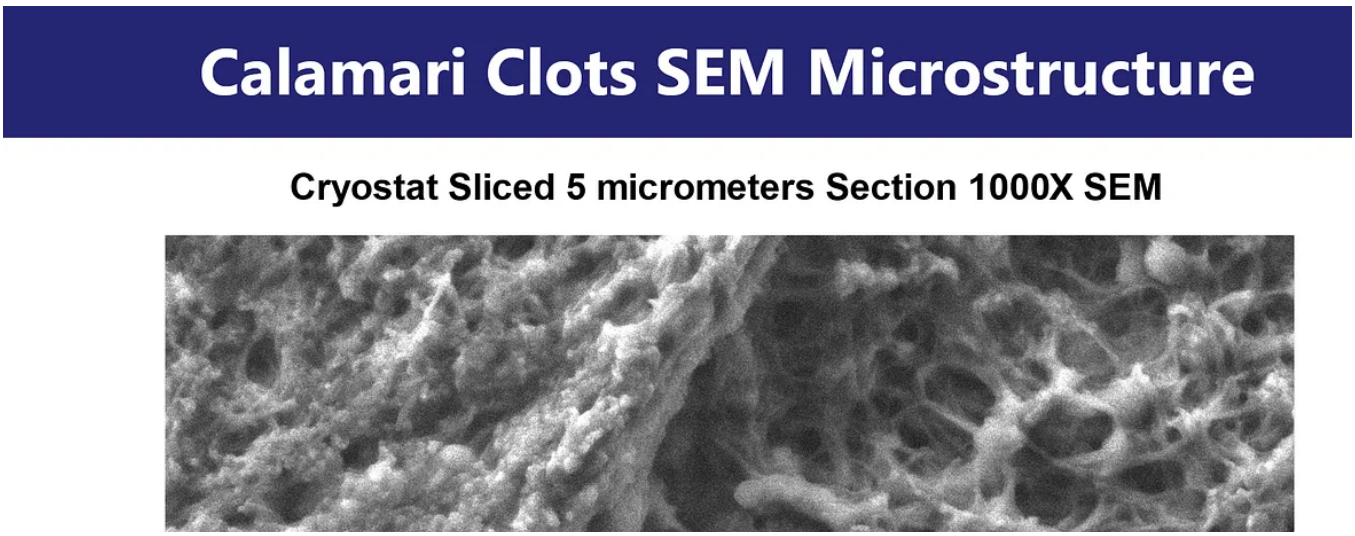

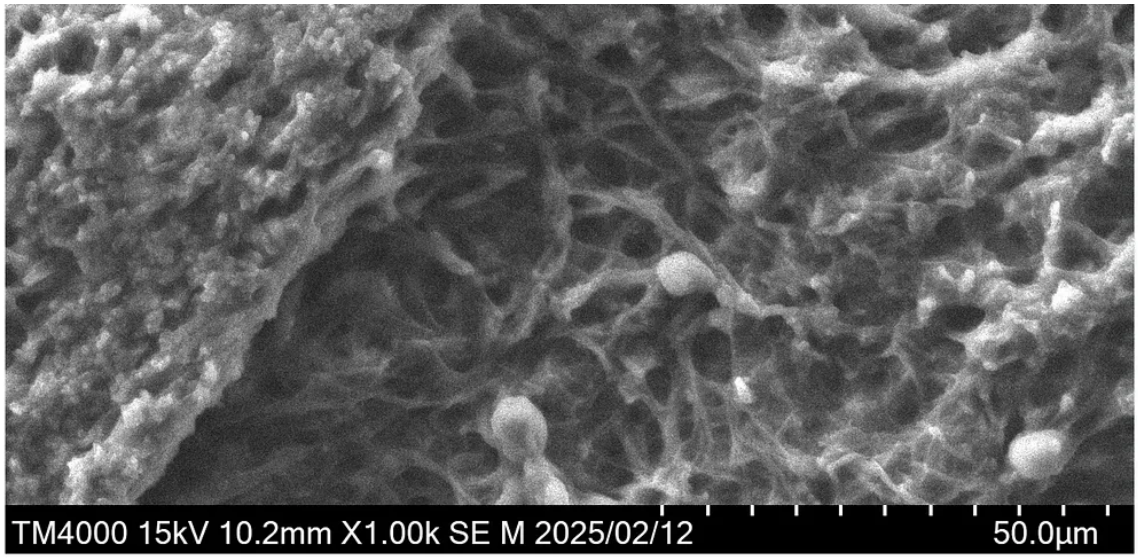

Slide 14: At 1000X magnification a complex topology, becomes apparent, linear forms can be seen to form branching interconnects of varying thickness, with globular forms also apparent. These structures are the fibrillar forms of amyloidogenic protein.

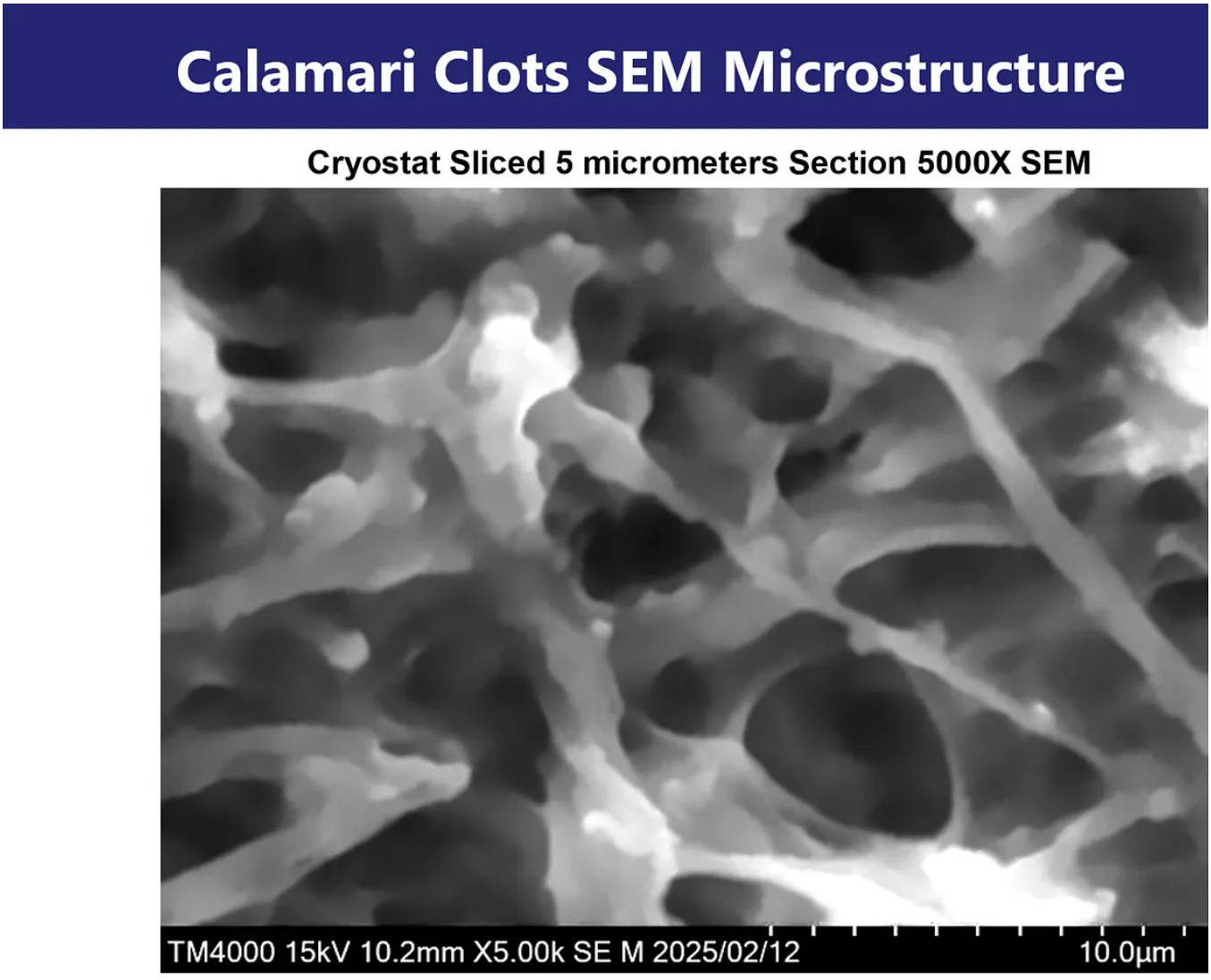

Slide 15: This high-magnification SEM image highlights the pathological

ultrastructure characteristic of amyloid fibrin formation. Central to the view is a primary fibril exhibiting a distinct, rapid rotational twist, indicative of abnormal helical pathology, often associated with protease resistance and altered mechanical properties. Surrounding the main fibril, numerous nodular and bulbous formations are visible, consistent with lateral aggregation and nucleation points typical of amyloidogenic remodeling. The exaggerated torsional features and nodular morphology reflect profound alterations from normal fibrin architecture, emphasizing the pathological assembly process associated with disease states.

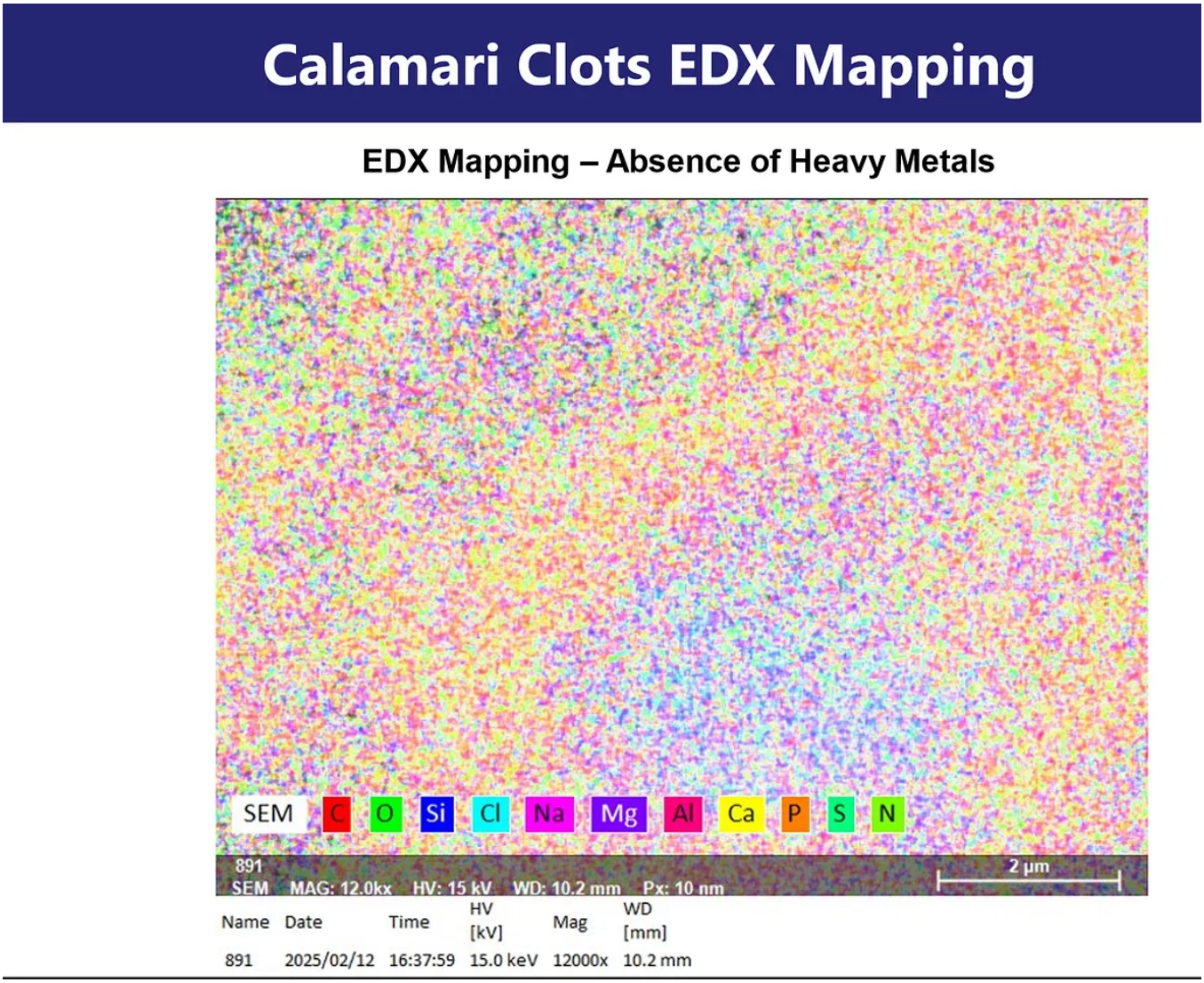

Slide 16: Spatial EDX mapping. This EDX map displays the spatial distribution of elemental composition across a fibrillar clot sample using SEM12,000× magnification. Each color corresponds to a specific element as indicated in the legend: carbon (C, red), oxygen (O, green), silicon (Si, blue), chlorine (Cl, cyan), sodium (Na, pink), magnesium (Mg, purple), aluminum (Al, magenta), calcium (Ca, yellow), phosphorus (P, orange), sulfur (S, light green), and nitrogen (N, lime). The widespread presence of carbon, oxygen, nitrogen, and sulfur suggests an organic matrix consistent with proteinaceous material. Notably, there is a lack of signal for transition or heavy metals (e.g., iron, zinc, copper, tin, or lead), implying that the fibrillar aggregation in this clot is not metal-driven. This distinguishes the composition from classic environmentally induced or metal-catalyzed pathological inclusions and supports a hypothesis of endogenous, possibly spike driven, protein

misfolding and deposition. The uniform distribution of biogenic elements (C, N, O, S, P) further reinforces the organic and likely proteinaceous origin of the structure.

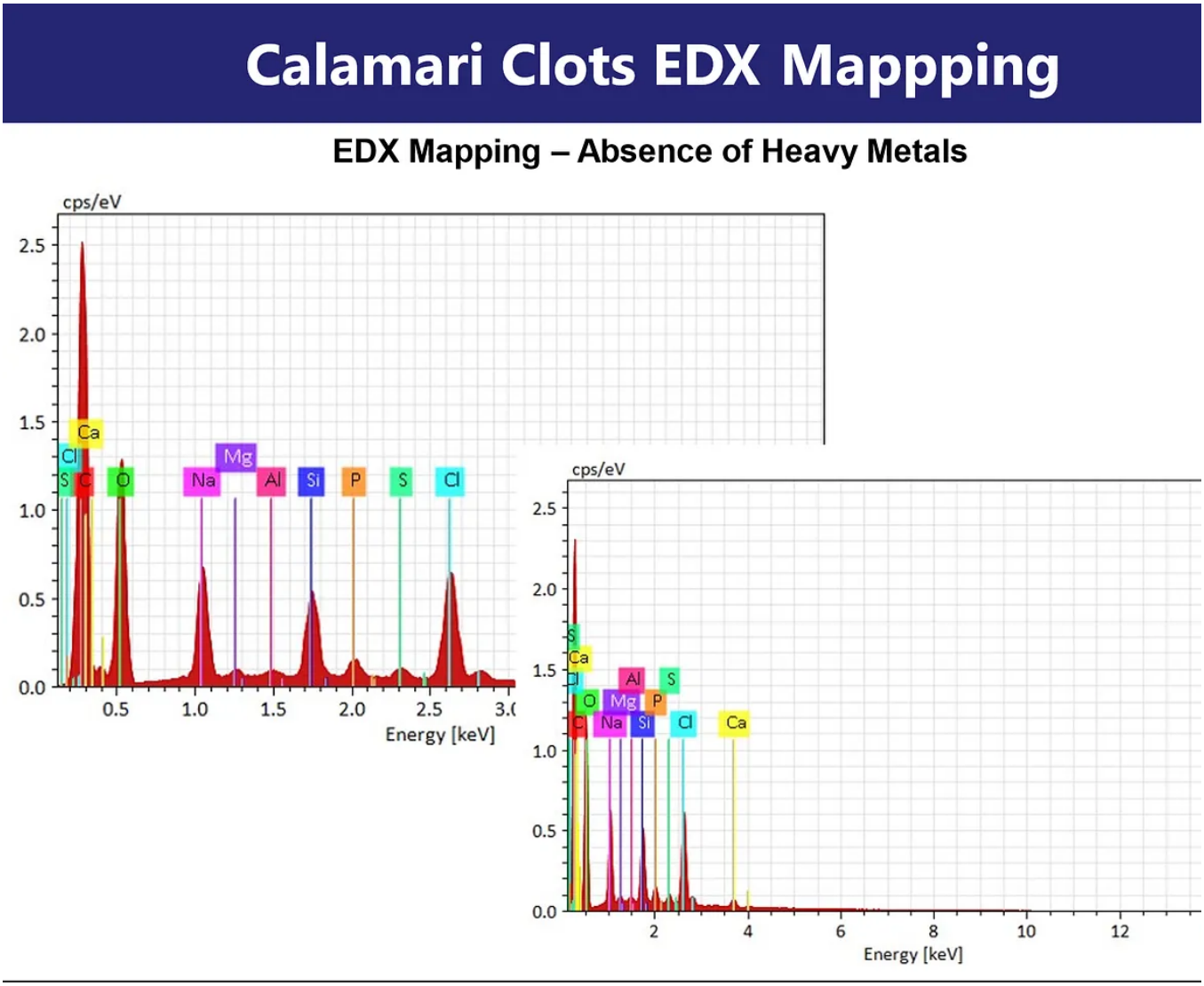

Slide 17: Quantitative EDX spectra of clot aggregates demonstrating elemental composition and absence of heavy or transition metals. EDX spectra reveals the predominance of light elements such as carbon (C), oxygen (O), sodium (Na), magnesium (Mg), phosphorus (P), sulfur (S), chlorine (Cl), potassium (K), and calcium (Ca). Notably, the absence of peaks corresponding to transition or heavy metals rules out contamination from environmental or industrial sources and suggests that the dense morphology is not due to mineralization. The abundance of Ca and Mg relative to trace elements may be relevant to charge stabilization or cross-linking mechanisms typical of amyloid fibrils. These findings support the interpretation that the clot aggregates are proteinaceous and not metal-derived in origin.

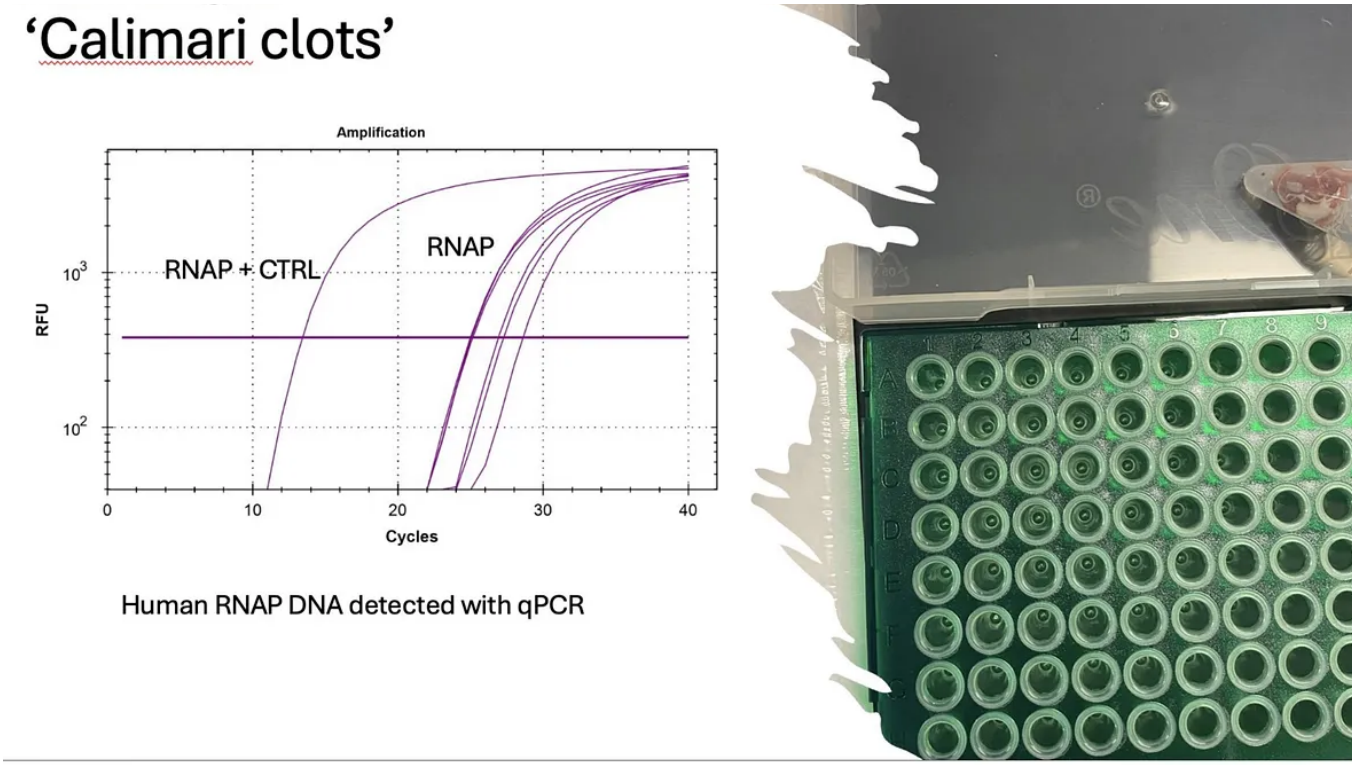

Slide 18; PCR Results for detection of human tissue using primers for detection of human RNA-Polymerase, this confirms that the tissue is of human origin

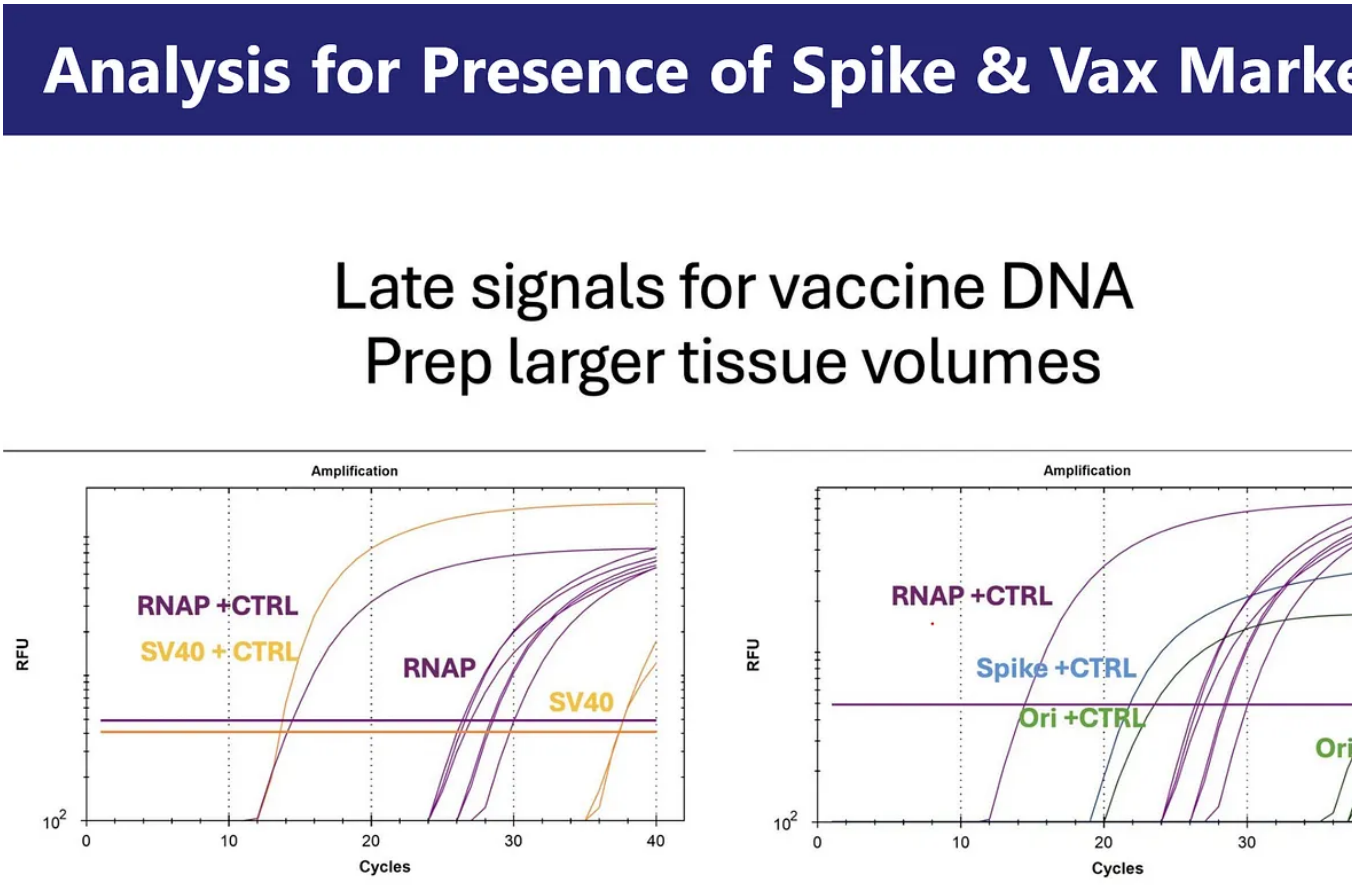

Slide 19: qPCR amplification plots demonstrating detection of human reference genes (RNAP), viral spike sequences, and plasmid vector markers (SV40 and Ori) from clot-derived tissue extracts. Amplification curves show positive detection of RNAP confirming the human origin of the sample. Late-cycle amplification signals for SV40 promoter, spike protein coding sequence, and Ori (origin of replication) suggest low-abundance presence of residual plasmid DNA consistent with LNP-based recombinant vaccine components. Controls were included for all primer sets. These results indicate preliminary molecular evidence for incorporation or association of spike vaccine-related material within the clot matrices.

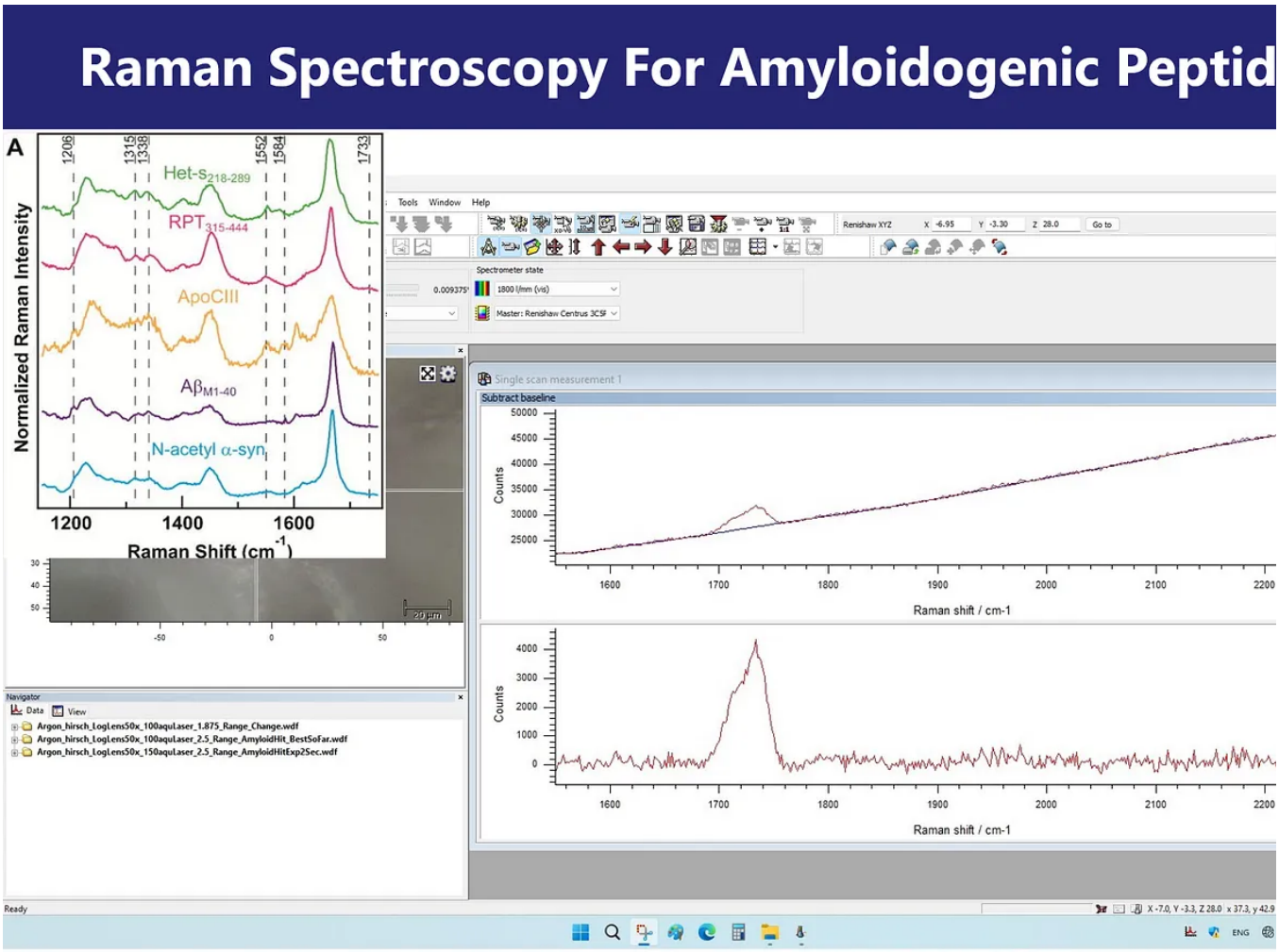

Slide 20 :Raman spectroscopy of clot-derived samples showing a shifted amyloid peak.Panel A (left inset) illustrates comparative Raman signatures for reference amyloidogenic proteins, including $A\beta_{1-40}$, ApoCIII, and α-synuclein (Flyn & Lee 2018). Spectra from clot-derived material (right panels – screen capture from Reinshaw WiRE) exhibit a prominent peak near 1720 cm^{-1}, deviating from the canonical β-sheet amyloid peak at ~1670 cm^{-1}. This spectral shift may indicate altered secondary structure, chemical modification, or complexation of the fibrils within the clot. The elevation in counts and sharpness of the signal confirm that amyloid burden is both present and conformationally distinct from standard protein

fibrils.

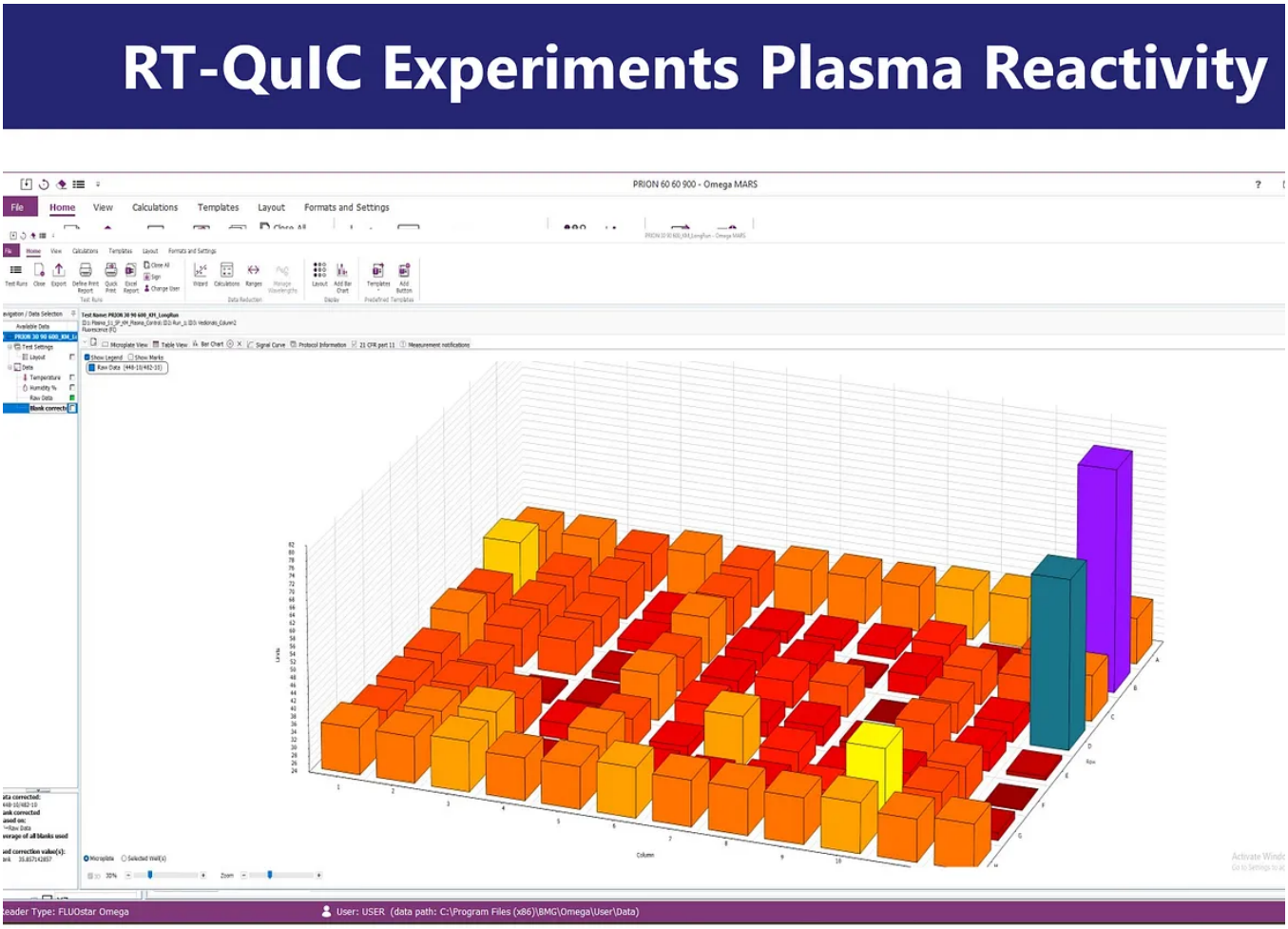

Slide 21: RT-QuIC plate reactivity heatmap for clot-derived plasma samples. 3D bar plot visualization of RT-QuIC assay output demonstrates spatial variation in sample reactivity across a 96-well plate (Screen Capture from BMG MARS Software). The vertical height and color saturation represent relative fluorescence intensity, indicative of ThT-binding to fibrillar products formed during the reaction. Elevated signals in two wells (B12 & D12) challenged with human plasma, the remaining wells are combination of various recombinant peptides in buffer solution); the specific reactive wells suggest seeding-competent material consistent with amyloidogenic or prion-like activity. Control wells (Rows A & H) remain low, supporting the specificity of reactivity to experimental samples. This assay provides preliminary evidence of templated misfolding activity within postmortem plasma fractions.

bumens@dingens.org Subscribe

Discussion about this post

Comments Restacks

>b Write a comment...

RexesRule RexesRule 1d

Dr. McCairn, thank you for your important and tireless work. Great to see an easy-to-shar summary here on Substack.

REPLY

Groovenuts Groovenuts's Substack 1d

Nice one Doc,

It's great to see a solid cohort of brilliant minds.

You haven't missed a beat when it comes to mapping out decent study concepts. I know i could click your fingers (funds pending) you'd take it to the next level, so here's to hoping

For the sake of all those with Long covid and Vaccine injuries I hope the world see's how i your work is.

Never give up!

REPLY

62 more comments...